



저작자표시-비영리-변경금지 2.0 대한민국

이용자는 아래의 조건을 따르는 경우에 한하여 자유롭게

- 이 저작물을 복제, 배포, 전송, 전시, 공연 및 방송할 수 있습니다.

다음과 같은 조건을 따라야 합니다:



저작자표시. 귀하는 원저작자를 표시하여야 합니다.



비영리. 귀하는 이 저작물을 영리 목적으로 이용할 수 없습니다.



변경금지. 귀하는 이 저작물을 개작, 변형 또는 가공할 수 없습니다.

- 귀하는, 이 저작물의 재이용이나 배포의 경우, 이 저작물에 적용된 이용허락조건을 명확하게 나타내어야 합니다.
- 저작권자로부터 별도의 허가를 받으면 이러한 조건들은 적용되지 않습니다.

저작권법에 따른 이용자의 권리는 위의 내용에 의하여 영향을 받지 않습니다.

이것은 [이용허락규약\(Legal Code\)](#)을 이해하기 쉽게 요약한 것입니다.

[Disclaimer](#)

전 용 필 교수 지도  
석사학위 청구논문

**Alternative Splicing  
of Yes-associated protein  
and its roles during implantation**

2025

성신여자대학교 대학원

생물학과

채 지 수

**Alternative Splicing  
of Yes-associated protein  
and its roles during implantation**

A Master's Thesis

Submitted to the

Graduate School of Sungshin University

In partial fulfillment of the requirements  
for the degree of master of biology

Ji Su Chae

November, 2024

This is certify that we have examined the  
Master's Thesis of  
Ji Su Chae  
Submitted to Department of Biology

Approved as to style and content:

Thesis Advisor



Yong pil Cheon

Committee Chairman



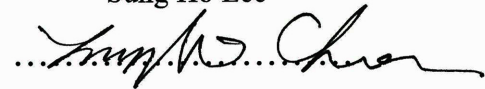
Byoung Joon Ko

Committee Member



Sung Ho Lee

Committee Member



Yong pil Cheon

The Graduate School of Sungshin University

# **ABSTRACT**

## **Alternative Splicing of Yes-associated protein and its roles during implantation**

Ji su Chae

Department of

Biology

Graduate School

Sungshin University

Decidualization is a vital process in early pregnancy, during which endometrial stromal cells undergo differentiation to support embryo implantation and facilitate developmental signaling.

The Hippo signaling pathway, a serine/threonine kinase cascade that regulates cell proliferation, survival, and apoptosis, is recognized as a critical factor in both normal development and pathological progression.

In this study, we examined the role of YAP1, the primary effector of the Hippo signaling pathway, in regulating decidualization during early pregnancy.

Western blot analysis of YAP1, its target gene CTGF, and the TEAD family transcription factors that interact with YAP1 demonstrated an increase in the expression of YAP1, CTGF, and TEAD1 as decidualization progressed.

Immunohistochemical analysis was performed from day 1 to day 7 of pregnancy to observe dynamic changes in YAP1 localization, which corresponded to physiological status.

Western blot analysis identified four distinct bands corresponding to alternative splicing isoforms of YAP1, with a significant increase observed on day 7 of pregnancy, which correlated with an increase in uterine size and weight.

In addition, higher expression of YAP1 was observed at the implantation site compared to the inter-implantation site. Subsequent analysis of post-

translational modifications (PTMs) revealed that the 60 kDa band corresponded to the glycosylated form of YAP1.

Further investigation using the O-GlcNAcAtlas 3.0 program confirmed that O-GlcNAcylation of mouse YAP1 occurs at serine 94, consistent with its human counterpart.

This suggests that O-GlcNAcylation may play a regulatory role in YAP1's function as a transcriptional co-activator. Furthermore, Western blot analysis of O-GlcNAcylated proteins in the uterus of early pregnant mice revealed a gradual increase in O-GlcNAcylation levels from day 1 to day 7 of pregnancy.

Co-immunoprecipitation (Co-IP) analysis confirmed that YAP1, represented by the 52 kDa and 28 kDa bands, interacts with O-GlcNAc. Collectively, these findings demonstrate that YAP1 plays a critical role in cell proliferation and differentiation in the early pregnant uterus and may regulate its physiological functions.

# CONTENTS

**Abstract (English)**

**Contents**

**List of Tables**

**List of Figures**

<b>Introduction</b> .....	<b>1</b>
<b>Materials and Methods</b> .....	<b>6</b>
Experimental animals .....	6
Total RNA extraction .....	6
cDNA synthesis .....	7
Real-time PCR analysis .....	7
Protein extraction and coomassie blue staining .....	8
Western blot .....	8
Immunoprecipitation .....	9
Immunohistochemistry .....	9
Protein deglycosylation .....	10
Protein extraction and digestion for mass spectrometry analysis ...	10
Sample clean-up and preparation for LC-MS/MS analysis .....	11
Statistics .....	12
<b>Results</b> .....	<b>16</b>

<b>Discussion .....</b>	<b>33</b>
<b>References .....</b>	<b>36</b>
<b>Abstract (Korean) .....</b>	<b>39</b>
<b>Acknowledgements .....</b>	<b>41</b>

## List of Tables

Table 1. Real-time RT-PCR Thermal cycler schedule .....	13
Table 2. Primer sequences for quantitative real-time PCR .....	14
Table 3. Antibody information .....	15
Table 4. Relative intensity of immunohistochemistry results .....	20
Table 5. O-GlcNAcylation sites in mouse YAP1 .....	31

## List of Figure

Figure 1. Structural analysis known spliced YAP1 in mouse .....	5
Figure 2. mRNA expression profiles of genes that main components of Hippo pathway .....	17
Figure 3. Tissue specific localization of YAP1 in mouse uterus during early pregnancy .....	19
Figure 4. Detection and identification of alternative splicing forms of YAP1 .....	22
Figure 5. Protein expression profiles of YAP1 during early pregnancy .....	25
Figure 6. Increase of the levels of YAP1 protein by implantation .....	27
Figure 7. Glycosylated YAP1 during pregnancy .....	29
Figure 8. YAP inhibition caused the delay of decidualization .....	32

## INTRODUCTION

Decidualization is a process during early pregnancy in which endometrial stromal cells at the implantation site undergo cellular morphological changes and functional differentiation to support embryo attachment and invasion, ultimately developing into the placenta that provides essential nutrients to the embryo. In mice, decidualization is initiated when the blastocyst enters the uterus on the fourth day post-fertilization (Paria et al., 1993; Wang & Dey, 2006). The blastocyst initiates the differentiation of stromal cells located beneath the attached uterine epithelium into decidual cells, characterized by increased cell size and altered secretory properties, forming the primary decidual zone (PDZ) by day five of pregnancy. By day eight of pregnancy, the decidual area expands to create the secondary decidual zone (SDZ), while the PDZ undergoes apoptosis and disappears. At this point, the number of decidual cells reaches its peak, after which regression of the decidua begins (He et al., 2021). This process is essential for successful pregnancy and involves a complex interplay of various hormones, transcription factors, cytokines, and signaling pathways.

The Hippo signaling pathway, first identified in *Drosophila*, regulates organ growth by controlling cell proliferation, survival, and apoptosis. This pathway is a serine/threonine kinase signaling cascade that is activated or inhibited by various hormones, growth factors, and mechanical stress. When the Hippo pathway receives signals from outside the cell, its key components Mammalian Ste20-like protein (MST) 1/2 kinase and Large tumor suppressor (LATS) 1/2 kinase are sequentially phosphorylated. LATS1/2 then phosphorylates the

transcription co-activator and main effector of the Hippo pathway, Yes-associated protein (YAP) 1 (Meng et al., 2016).

When YAP1 is phosphorylated, it binds to 14-3-3 proteins, leading to its retention in the cytoplasm or degradation, thereby becoming inactive. In contrast, when the Hippo pathway is turned off, LATS1/2 kinase remains inactive and is unable to phosphorylate YAP1. Consequently, the unphosphorylated YAP translocates to the nucleus, where it associates with transcription factors to activate the transcription of target genes (Meng et al., 2016).

YAP1 does not have direct DNA-binding sites; therefore, it must associate with DNA-binding transcription factors to activate transcription. The target genes that YAP1 activates vary depending on the transcription factors it binds to, which ultimately determine its function. A prominent partner of YAP1 is the TEA domain transcription factor (TEAD) family, which includes transcription factors such as connective tissue growth factor (CTGF) that promote cell proliferation and regulate the cell cycle (Chen et al., 2019). Additionally, YAP1 can interact with several transcription factors, such as Runx and ErbB4, that possess a PPxY motif, which binds to the WW domain of YAP1 (Kim et al., 2018).

Alternative splicing is an essential mechanism that increases the complexity of gene expression by altering the composition of exons and introns in the primary transcript, resulting in the production of proteins with diverse functions. In humans, eight alternative splicing forms of YAP1 have been identified (Sudol, 2013), and a similar number of eight splicing forms are known in mice (Xu et al., 2021).

As shown in Figure 1, YAP1 is composed of several domains. The N-terminal region contains a TEAD binding domain (TBD) that allows for interaction with the TEAD family, while the C-terminal region features a transactivation domain that plays a crucial role in transcriptional activation, although it does not directly bind transcription factors. Between these two regions are two WW domains that can interact with the PPxY motif (Zhao et al., 2009). According to the currently identified alternative splicing forms of mouse YAP1, the loss of exon 1 and part of exon 3 is expected to result in the absence of the first WW domain, and the deletion of part of exon 6 is anticipated to impair the transactivation domain (Vassilev et al., 2001).

If alternative splicing forms occur as modifications after transcription, then post-translational modifications (PTMs) include phosphorylation, acetylation, and glycosylation. Phosphorylation, in particular, is a mechanism that regulates YAP1 activity, as specific serine and threonine residues of YAP1 are phosphorylated by LATS1/2, leading to the suppression of its transcriptional activity. Glycosylation has also been shown to affect YAP1's transcriptional activation, with one form, O-GlcNAcylation, being a modification where a single O-GlcNAc is attached to the serine or threonine residues of a protein by O-GlcNAc transferase (OGT). O-GlcNAcylation occurs more readily at higher glucose concentrations and is a dynamic process, making it more closely influenced by the nutritional status of the cell compared to O-glycosylation (Mannino & Hart, 2022). In humans, YAP1 has been found to undergo O-GlcNAcylation at S109 and T241. When YAP1 is O-GlcNAcylated, it competes with the phosphorylation sites targeted by LATS1/2 or indirectly inhibits phosphorylation, thereby enhancing YAP1's transcriptional activity (Meng et al., 2016; Peng et al., 2017). In a previous study, it was observed that the level of O-GlcNAc protein modification was higher in the secretory phase, i.e., the

receptive phase, of human endometrial tissue compared to the proliferative phase. Moreover, when O-GlcNAc transferase (OGT) and O-GlcNAcase (OGA) were knocked down to regulate the O-GlcNAcylation level, it was found that an increase in O-GlcNAcylation significantly enhanced the degree of embryo attachment, cell proliferation, and migration in an endometrial cell line. Therefore, it is anticipated that O-GlcNAcylation plays a crucial role in regulating protein function during embryo implantation (Han et al., 2019).

YAP1 has been found to be expressed in the mouse endometrium (Moon et al., 2022), with higher levels observed in the decidua of pregnant women compared to the endometrium of non-pregnant women (Chen et al., 2017). Furthermore, experimental studies have shown that inactivation of YAP during the process of decidualization in mice impairs the proliferation and differentiation of stromal cells, leading to DNA damage and resulting in abnormal decidualization (Yu et al., 2022). However, previous studies have shown that there is no significant difference in decidual response between AMHR-based conditional YAP1 null mice and wild-type mice when artificial decidual induction is performed (Godin et al., 2020), suggesting that the role of YAP1 during pregnancy remains controversial. Decidualization are confused via various factor and YAP1 also suspected one. However, the molecular mechanism and processes are not much uncovered.

So, in this study, we investigate the role of YAP1 in pregnancy along with splicing of YAP1, and the impact of YAP1 glycosylation.

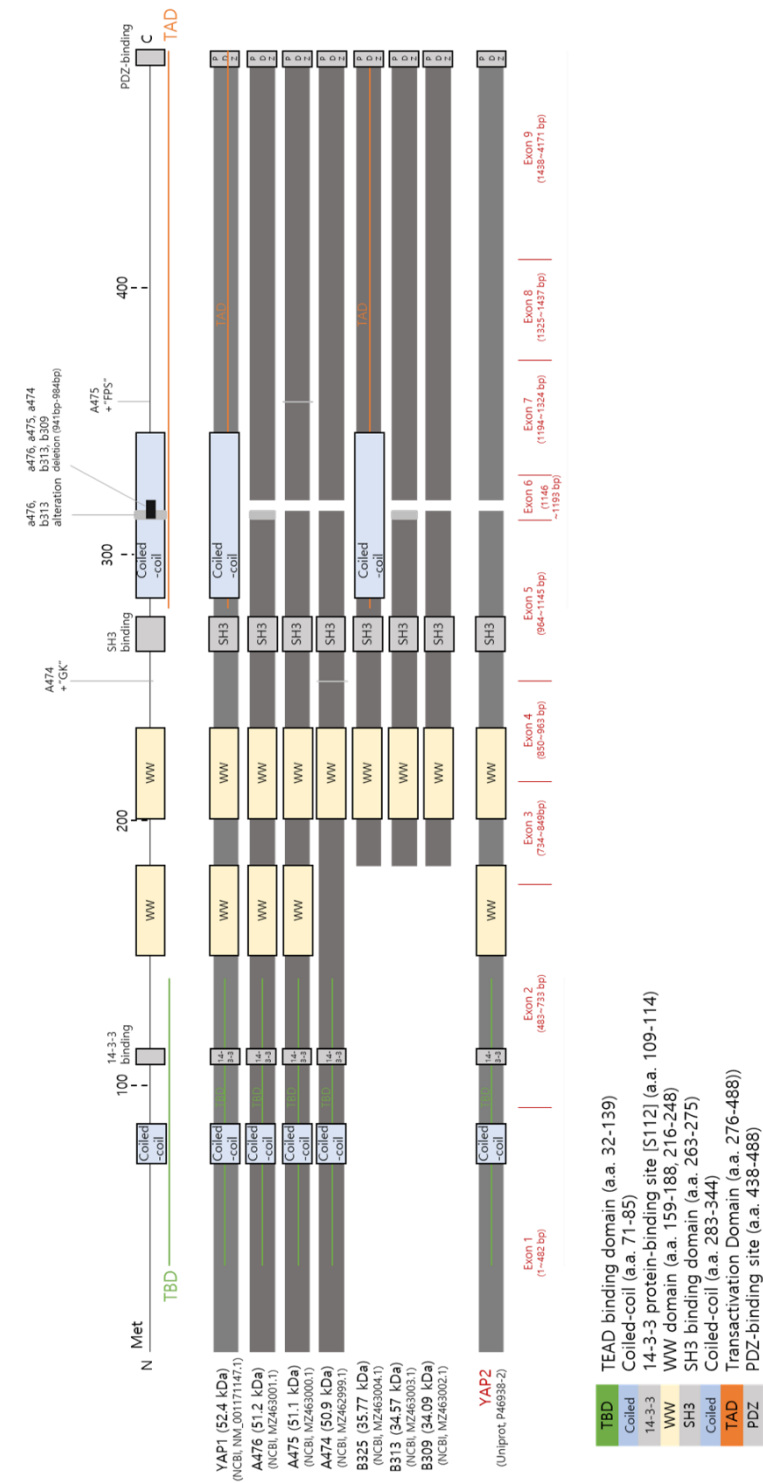


Figure 1. Structural analysis known spliced YAP1 in mouse.

## **MATERIALS AND METHODS**

### **Experimental animals**

All animal experiments were conducted in accordance with the Guide for the Care and Use of Laboratory Animals published by the National Institutes of Health (NIH). The studies were approved by the Institutional Animal Care and Use Committee (IACUC) at Sungshin Women's University (SSWIACUC-2024-006). 6-8-week-old ICR mice were housed under a controlled light cycle, with lights on at 6:00 AM and off at 7:00 PM, in a clean room environment. Mice were given access to standard rodent chow and water ad libitum starting at 28 days of age, after weaning. To obtain uterine tissue from specific stages of pregnancy, female mice were mated with fertile wild-type males, and the presence of a vaginal plug was designated as Pregnant Day 1 (PD1).

### **Total RNA extraction**

The uterus was homogenized in TRIzol<sup>®</sup> reagent (Invitrogen, Cat #: 15596-026, Massachusetts, USA) at a ratio of 1 ml per 0.1 g of tissue and incubated for 10 minutes at room temperature (RT). Then, 0.2 ml of chloroform per 1 ml of TRIzol was added to the homogenized sample, which was shaken vigorously for 15 seconds and left at RT for 15 minutes. The mixture was then centrifuged at 12,000 g for 15 minutes at 4°C. The resulting supernatant was transferred to a new tube, and 0.5 ml of isopropanol was added to each 1 ml of TRIzol. The sample was mixed gently and incubated at RT for 10 minutes. Afterward, the

sample was centrifuged at 12,000 g for 8 minutes at 4°C. The supernatant was removed, and the RNA pellet was washed by gently inverting the tube in 1 ml of 75% ethanol, followed by centrifugation at 7,500 g for 5 minutes at 4°C. The supernatant was discarded, the pellet was air-dried for 20 seconds at RT to remove ethanol, and 50 µl of 0.1% DEPC-treated water was added to dissolve the RNA.

### **cDNA synthesis**

Briefly, the reaction mixture consisted of 26.5 µl of total RNA, 10 µl of MMLV 5X buffer, 1 µl of oligo dT primer (0.5 µg/µl), 1 µl of random primer (0.1 µg/µl), and 4 µl of dNTP mix (100 mM). The reaction was incubated at 65°C for 5 minutes, then allowed to cool to room temperature for 10 minutes. Next, 4.5 µl of DTT (100 mM), 2 µl of M-MLV Reverse Transcriptase (Promega, Cat#: M170B, Wisconsin, USA), and 1 µl of RNase block ribonuclease inhibitor (40 U/ml) were added. The reaction was then incubated at 42°C for 1 hour and terminated by heating at 70°C for 10 minutes to stop cDNA synthesis. The final product was stored at -20°C until use.

### **Real-time PCR analysis**

To quantify gene expression, target gene transcripts were amplified by reverse transcription (RT)-PCR using specific primers (Table 2). Quantitative real-time RT-PCR was carried out with SYBR Premix Ex Taq™ (TaKaRa, #RR420, Japan) on an AriaMx Real-time PCR System (Agilent, #G8830A, USA). Details of the thermal cycling conditions are provided in Table 1. Each reaction was performed in

triplicate, with 1  $\mu$ l of cDNA in each well. Dissociation curves were generated for all reactions to confirm amplification of a single product with the correct melting temperature. Gene expression fold change was calculated using the  $\Delta\Delta$ Ct method, with the ribosomal protein 36B4 as the internal control.

### **Protein extraction and coomassie blue staining**

The uterus was homogenized in cold homogenization buffer containing 50 mM Tris-Cl, 150 mM NaCl, 10 mM  $\beta$ -mercaptoethanol, 2 mM CaCl<sub>2</sub>, 0.1 mM PMSF, 1  $\mu$ M Leupeptin, 1  $\mu$ M Pepstatin, 0.5 mM EDTA, 15% Glycerol, and 0.1% NP-40. The resulting homogenate was centrifuged to remove insoluble debris. Protein concentration was measured using a BCA assay (Thermo Fisher Scientific, #23225, USA). A protein sample of 30  $\mu$ g/ml was boiled with SDS/ $\beta$ -mercaptoethanol sample buffer and loaded onto a 10% SDS-PAGE gel. Proteins were separated by electrophoresis. After the SDS-PAGE run, the gel was stained with Coomassie Blue solution (0.1% Coomassie Brilliant Blue R250, 50% methanol, 10% glacial acetic acid in distilled water) for 2 hours, then incubated in a destaining solution while shaking overnight.

### **Western blot**

Following SDS-PAGE, proteins were transferred onto polyvinylidene difluoride (PVDF) membranes (Bio-Rad, #1620177, USA) using transfer buffer containing 25 mM Tris base, 192 mM Glycine, 0.1% SDS, and 20% Methanol. The membranes were blocked with 10% skimmed milk in TBST buffer (10 mM Tris-HCl, 150 mM NaCl, and 0.05% Tween-20) for 1 hour at room temperature (RT), then washed three times with TBST. The membranes were incubated overnight

at 4°C with the primary antibody (Table 3). After washing three times, membranes were incubated with goat anti-mouse IgG-HRP (diluted 1:2000) for 1 hour. Bands were visualized using ECL solution (Bio-Rad, #1705060, USA) and detected with the ChemiDoc MP Imaging System (Bio-Rad, #17001402, USA). Band intensities were quantified and normalized to total protein levels using ImageJ software.

### **Immunoprecipitation**

Protein sample (500 µg) was rotated with mouse monoclonal YAP1 antibody (5 µg) and homogenization buffer 500 µl (50 mM Tris-Cl, 150 mM NaCl, 10 mM β-mercaptoethanol, 2 mM CaCl<sub>2</sub>, 0.1 mM PMSF, 1µM Leupeptin, 1 µM Pepstatin, 0.5 mM EDTA, 15% Glycerol, and 0.1% NP-40) for overnight. And after the addition of 50 µl Protein A/G–Agarose (Santa cruz Biotechnology, SC-2003, USA), sample was rotated at 4°C for 2 hr. Then centrifuged 12,000 g for 2 min at 4°C. The supernatant was removed and rotated for 5 min after adding 1ml homogenization buffer. Repeat four times from centrifuge. The supernatant was removed and added 20 µl SDS/β-mercaptoethanol sample buffer. Sample was boiled at 95°C for 5 min for elution.

### **Immunohistochemistry**

4 µm tissue sections were mounted on glass slides and subjected to antigen retrieval by incubating in boiling 10 mM sodium citrate buffer (pH 6.0) for 15 minutes. Endogenous peroxidase activity was blocked by treating the sections with 0.3% hydrogen peroxide in water for 5 minutes. YAP immunoreactivity was detected using the VECTASTAIN® Elite ABC-HRP kit, Peroxidase (Mouse IgG) (Vector Laboratories, Cat #PK-6102, California, USA). In brief, the tissues were

incubated with 1% normal horse serum in 0.1% BSA in PBS for 1 hour to block non-specific binding. Following this, the sections were incubated with mouse monoclonal YAP antibody (diluted 1:200) in 0.1% BSA in PBS for 1 hour. After washing with PBST and PBS, tissues were incubated with avidin-biotin complex reagent containing horseradish peroxidase for 30 minutes. After additional washes with PBST and PBS, color development was achieved using DAB substrate (Vector Laboratories, Cat #SK-4100, California, USA). The sections were then counterstained with hematoxylin.

### **Protein deglycosylation**

Total protein from mouse uterine tissue (190 µg) was diluted to a final volume of 40 µL using protein lysis buffer. Subsequently, 5 µL of deglycosylation mix buffer 2 (NEB, Cat #B6045, USA) was added, and the mixture was incubated at 75°C for 10 minutes. Following this, 5 µL of protein deglycosylation mix II (NEB, Cat #P6044, USA) was added, and the solution was gently mixed. The reaction was then allowed to proceed at room temperature for 30 minutes, followed by a further incubation at room temperature for 16 hours.

### **Protein extraction and digestion for mass spectrometry analysis**

Total proteins were extracted from the uterus of pregnant mice and separated by SDS-PAGE. The gel was stained with Coomassie blue solution. The corresponding bands were identified by comparing the results with YAP1 Western blot data, and the relevant sections of the gel were excised. The excised gel pieces were cut into small fragments and placed in for destaining. The gel pieces were then dehydrated by replacing the solution with 100% acetonitrile.

Following dehydration, the gel pieces were incubated with 10 mM DTT in 25 mM ammonium bicarbonate at 56°C for 1 hour at 600 rpm. Afterward, the gel pieces were transferred to a solution of 55 mM iodoacetamide in 25 mM ammonium bicarbonate and incubated in the dark at 56°C for 1 hour at 600 rpm. The gel was washed with 100% acetonitrile and then dehydrated by replacing with 100% acetonitrile. The gel pieces were then incubated with 12.5 ng/μl trypsin in 25 mM acetonitrile at 4°C for 40 minutes, followed by washing with 25 mM ammonium bicarbonate. Afterward, the gel pieces were incubated with 50 mM ammonium bicarbonate at 37°C overnight with shaking. After the incubation, the supernatant was collected by centrifugation, and the gel pieces were incubated with 25 mM ABC in 50% acetonitrile at 37°C and 600 rpm for 15 minutes. Next, the samples were sonicated for 5 minutes at 37°C, and the supernatant was collected again after centrifugation. The collected extraction solution was vacuum-dried using a speed vac.

### **Sample clean-up and preparation for LC-MS/MS analysis**

The Sep-Pak Vac C18 1cc cartridge was activated with 100% acetonitrile, followed by equilibration with solvent A (5% acetonitrile + 0.1% formic acid in D.W.). The sample (10% in solvent A) was loaded onto the cartridge, and solvent A was passed through to wash the cartridge. Elution was performed with elution buffer (70% acetonitrile in D.W.), and the eluate was collected. The samples were then vacuum-dried using a speed vac and analyzed by LC-MS/MS (Waters, Xevo G2-XS QToF). Data processing was carried out using the Unifi program.

## **Statistics**

All experiments were performed at least three times. Statistical significance between the control and experimental groups was assessed using the Student's t-test. Data are expressed as the mean  $\pm$  standard error of the mean (SEM). A p-value of less than 0.05 was considered statistically significant. All statistical analyses were carried out using IBM SPSS Statistics software.

**Table 1. Real-time-PCR Thermal cycler schedule**

<b>Step</b>	<b>Temperature(°C)</b>	<b>Time</b>	<b>cycles</b>	
<b>Hold</b>	94	30 min	1	
	Denaturation	95	1 min	
<b>3 steps PCR</b>	Annealing	59	30 sec	45
	Extension	72	1 min	
	Denaturation	95	15 sec	
<b>Dissociation</b>	Annealing	60	30 sec	1
	Extension	95	15 sec	
<b>Hold</b>	4	Indefinitely	1	

**Table 2. Primer sequences for real-time PCR**

Gene	Symbol	NCBI gene reference	Primer sequence (5'-3')	Amplified length (bp)
Yes-associated protein 1	<b><i>YAP1</i></b> (exon 1)	NM_001171147.1	S GACTTGGAGGGCTCTTCAAT	193
			AS GAACATGCTGTGGAGTCAGAGCT	
Yes-associated protein 1	<b><i>YAP1</i></b> (exon 3)	NM_001171147.1	S GCTTTGGCAACTGAACGTTCTT	204
			AS GTGATCCTCTGGTTTCATGGCAAA	
WW domain containing transcription regulator 1	<b><i>Wwtr1</i></b> ( <i>TAZ</i> )	NC_001168281.1	S TCGCAGGAACTTGCCTTACA	231
			AS TTCCTGGACCAAGCTGCCTA	
TEA Domain Transcription Factor1	<b><i>Tead1</i></b>	NC_001166584.2	S ATCCATTGGCACACCAAGC	211
			AS GCCCTTCCAAAACAGCTCCTC	
Connective tissue growth factor	<b>CTGF</b>	NM_010217.2	S TTGGCCCAGACCCCAACTATG	232
			AS TTGACAGGCTTGGCGATTTT	
60S acidic ribosomal protein P0	<b><i>Rplp0</i></b> ( <i>m36B4</i> )	NM_007475.5	S CGACCTGGAAGTCCAACTACTTCCT	303
			AS GCACCTTATTGGCCCAACAGCAT	

**Table 3. Antibody information**

<b>Antibody</b>	<b>Description</b>	<b>Cat #</b>	<b>Company</b>
YAP (H-9)	Mouse monoclonal	SC-271134	SANTA CRUZ
TEAD1	Rabbit monoclonal	12292s	Cell signaling
p-YAP	Rabbit polyclonal	Orb99152	Biorbyt
O-GlcNAc	Mouse monoclonal	Ab2739	abcam

## RESULTS

### **mRNA expression profiles of genes that main components of Hippo pathway**

To investigate the involvement of the Hippo pathway in the uterus during early pregnancy, the mRNA expression levels of YAP1, the main effector of the Hippo pathway, TAZ (the homologue of YAP1), the main downstream gene CTGF, and the TEAD family transcription factors (TEAD1, 2, 3, 4), which interact with YAP1, were measured using qRT-PCR in the uteri of pregnant mice (Fig. 2).

YAP1 expression increased until day 3 of pregnancy, then decreased on day 4, before rising again on day 7. Notably, during decidualization from days 5 to 7, there was a significant increase in YAP1 expression (Fig. 2A). TAZ also showed an increase starting on day 4, with a significant rise on days 6 and 7. Among the TEAD family, TEAD1 exhibited a significant increase during decidualization, suggesting that TEAD1 may play a functional role during decidualization in mice (Fig. 2C). Although CTGF showed a significant increase on day 3, it did not reach statistical significance (Fig. 2G).

These results suggest that YAP1 may play a role during decidualization, and TEAD1, a transcription factor that interacts with YAP1, is likely to be involved in this process.

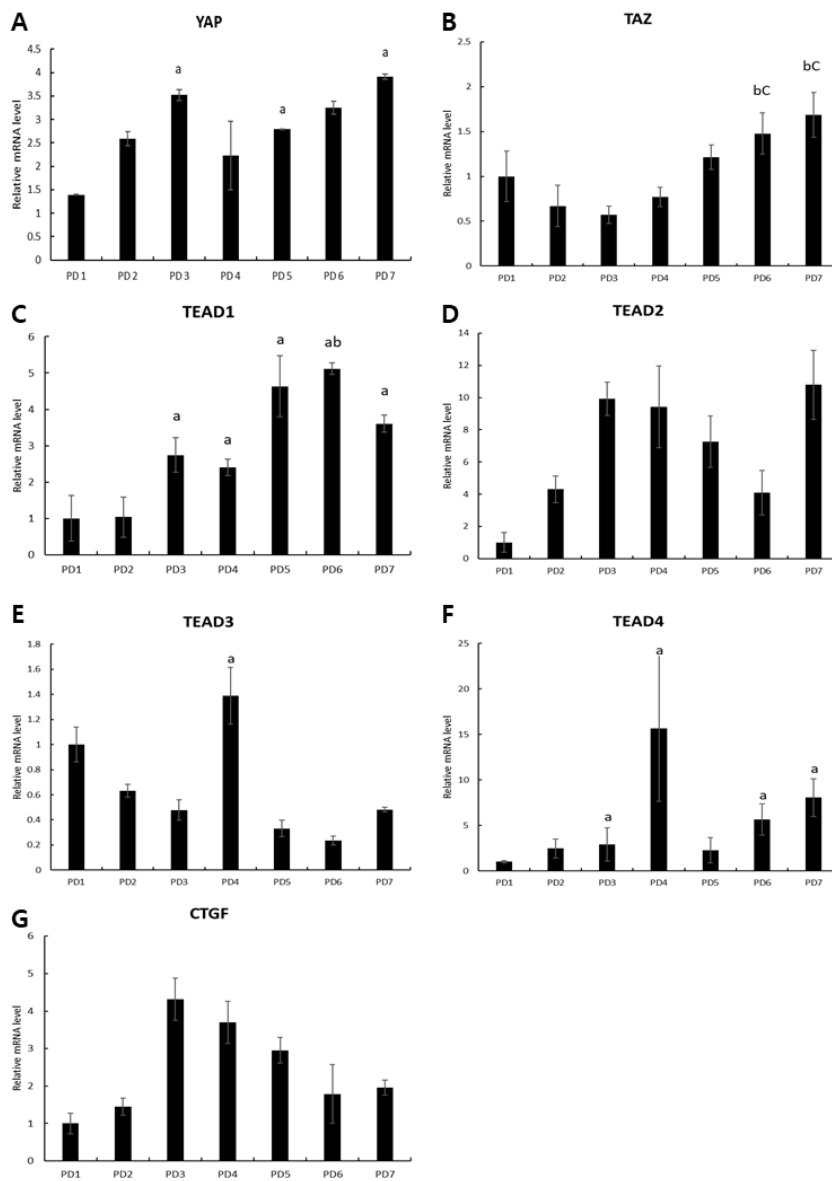


**Figure 2. mRNA expression profiles of genes that main components of Hippo pathway.**

Western blot analysis of mouse uterus in pregnant day 1 to 7. Genes expression was measured by RT-qPCR. mRNA level was calculated using the  $\Delta\Delta C_t$  method with the 36B4, as the internal control. PD: pregnant day. a:  $p < 0.05$  (a significant difference vs PD1). b:  $p < 0.05$  (a significant difference vs PD2). c:  $p < 0.05$  (a significant difference vs PD3).

### **Tissue specific localization of YAP1 in mice uterine cell during early pregnancy**

To investigate the expression pattern of YAP1 in the uterus of mice during decidualization, uterine tissues from pregnant mice on days 1 through 7 were collected and analyzed by immunohistochemistry (Fig. 3). From day 1 to day 4 of pregnancy, before implantation, YAP1 was primarily localized in the luminal epithelial and glandular epithelial cells. On day 5 of pregnancy, as decidualization began, the primary decidual zone (PDZ), where cell proliferation and differentiation occur, was formed, starting from the antimesometrial PDZ, where implantation takes place. Subsequently, apoptosis in the PDZ led to the formation of the secondary decidual zone (SDZ) in a broader area, with further cell proliferation and differentiation.

Immunohistochemistry results also showed that on day 5, the highest expression of YAP1 was observed in the antimesometrial primary decidual zone, the site where decidualization begins. On day 6, YAP1 expression was highest in the mesometrial primary decidual zone and the antimesometrial secondary decidual zone, and on day 7, the highest expression was observed in the mesometrial secondary decidual zone (Table 4). These findings indicate that the localization of YAP1 follows the progression of decidualization.

Thus, these results suggest that YAP1 plays a crucial role in the formation of the decidualization zones in the mouse uterus.

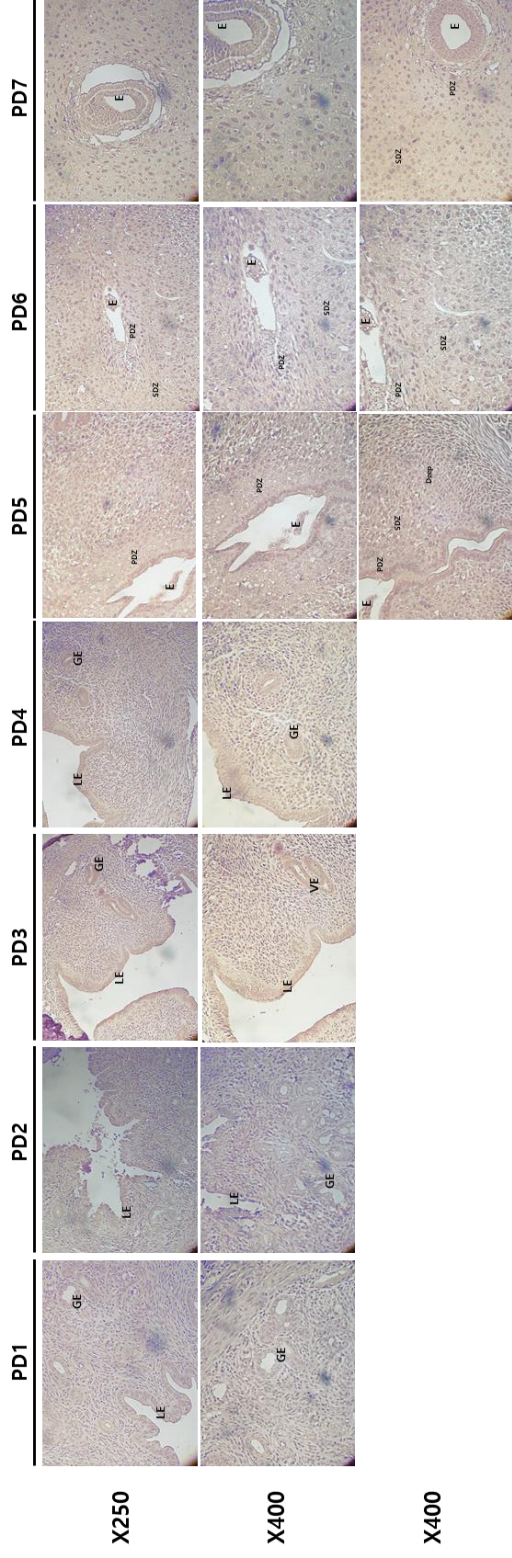


**Figure 3. Tissue specific localization of YAP1 in mice uterine cell during early pregnancy.**

The expression of YAP1 in pregnant mouse endometrium was histologically compared. LE: luminal epithelia, GE: Glandular epithelia, VE: vesicular epithelia E: embryo, PDZ: primary decidual zone, SDZ: secondary decidual zone.

**Table 4. Relative intensity of immunohistochemistry results.**

Quantification of immunohistochemistry results was performed using ImageJ, and relative expression levels are indicated with a '+' symbol.

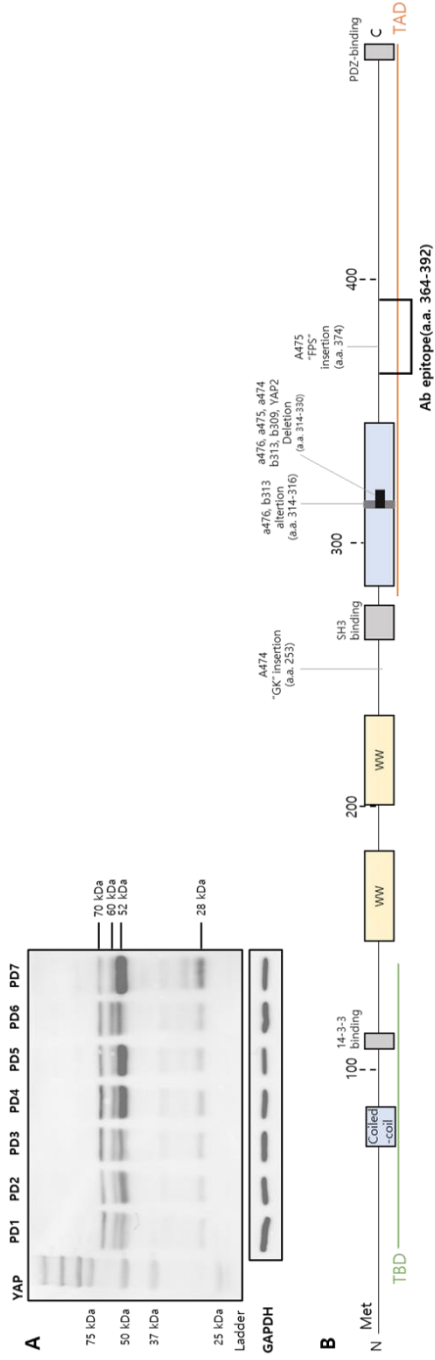
		PD 5	PD 6	PD 7
<b>Mesometrium</b>	PDZ	++	+++	+
	SDZ	+	+++	+++
	Deep	+	+	++
<b>Antimesometrium</b>	PDZ	+++	+	+
	SDZ	++	++	++
	Deep	+	+	++

### **Detection and identification of alternative splicing forms of YAP1**

Western blotting was performed using an antibody that detects the 364-392 amino acid region of mYAP1 on uterine proteins from days 1 to 7 (PD1-7).

When the binding site of the antibody used in the Western blot was BLASTed, the only protein that matched 100% was YAP1. The antibody was used to detect the amino acid sequences present in all the isoforms shown in Figure 1 (Fig. 4A).

Four clearly visible bands were obtained using in-gel digestion, and their sequences were compared and analyzed with the YAP1 sequence through LC-MS/MS (Fig. 4B-E). The analysis confirmed that all four bands corresponded to YAP1.



**D #YAP (60 kDa)**

Identified 6%	Chain 1 (10% coverage)
1:1 to 90	REPAQPPQ PARGGAPPS VSPAGTAP PAPPAGQV HWGQSEIDL EALFNAMWP KLNQWQVTP MLEKLDQSF FPFPEKSKS
1:91 to 195	TTTQDPKRA RLSQLWVAP ASFAVPTLM NSASGPIIDG MEQANTDQE VYTIHMKET TSHLDPLDP REANNAITQ SAAWQPPPL YAP
1:271 to 360	APQSQGVVL GGGSSNQKQD IQLQQLQEK ERLRGGSEL QVATIRHP STAMPACQE LALESQVPTL EQDGGTPAV SPSGASQELR YAP
1:361 to 460	TRHTSSGPF LNSGTYNSRD ESTDSGLSKS SYSPRTPDD FLUSVDHDT GOTTSQSTLP SQQSRFPDVL EALPCTINVL GTLEGDAMI
1:461 to 488	EGEELPSPQL DALSSLELQV ESNLAATKLD KESFLTW

**C #YAP (70 kDa)**

Identified 3%	Chain 1 (6% coverage)
1:1 to 90	REPAQPPQ PARGGAPPS VSPAGTAP PAPPAGQV HWGQSEIDL EALFNAMWP KLNQWQVTP MLEKLDQSF FPFPEKSKS
1:91 to 195	TTTQDPKRA RLSQLWVAP ASFAVPTLM NSASGPIIDG MEQANTDQE VYTIHMKET TSHLDPLDP REANNAITQ SAAWQPPPL YAP
1:271 to 360	APQSQGVVL GGGSSNQKQD IQLQQLQEK ERLRGGSEL QVATIRHP STAMPACQE LALESQVPTL EQDGGTPAV SPSGASQELR YAP
1:361 to 460	TRHTSSGPF LNSGTYNSRD ESTDSGLSKS SYSPRTPDD FLUSVDHDT GOTTSQSTLP SQQSRFPDVL EALPCTINVL GTLEGDAMI
1:461 to 488	EGEELPSPQL DALSSLELQV ESNLAATKLD KESFLTW

**F #YAP (28 kDa)**

Identified 2%	Chain 1 (4% coverage)
1:1 to 90	REPAQPPQ PARGGAPPS VSPAGTAP PAPPAGQV HWGQSEIDL EALFNAMWP KLNQWQVTP MLEKLDQSF FPFPEKSKS
1:91 to 195	TTTQDPKRA RLSQLWVAP ASFAVPTLM NSASGPIIDG MEQANTDQE VYTIHMKET TSHLDPLDP REANNAITQ SAAWQPPPL YAP
1:271 to 360	APQSQGVVL GGGSSNQKQD IQLQQLQEK ERLRGGSEL QVATIRHP STAMPACQE LALESQVPTL EQDGGTPAV SPSGASQELR YAP
1:361 to 460	TRHTSSGPF LNSGTYNSRD ESTDSGLSKS SYSPRTPDD FLUSVDHDT GOTTSQSTLP SQQSRFPDVL EALPCTINVL GTLEGDAMI
1:461 to 488	EGEELPSPQL DALSSLELQV ESNLAATKLD KESFLTW

**E #YAP (52 kDa)**

Identified 2%	Chain 1 (4% coverage)
1:1 to 90	REPAQPPQ PARGGAPPS VSPAGTAP PAPPAGQV HWGQSEIDL EALFNAMWP KLNQWQVTP MLEKLDQSF FPFPEKSKS
1:91 to 195	TTTQDPKRA RLSQLWVAP ASFAVPTLM NSASGPIIDG MEQANTDQE VYTIHMKET TSHLDPLDP REANNAITQ SAAWQPPPL YAP
1:271 to 360	APQSQGVVL GGGSSNQKQD IQLQQLQEK ERLRGGSEL QVATIRHP STAMPACQE LALESQVPTL EQDGGTPAV SPSGASQELR YAP
1:361 to 460	TRHTSSGPF LNSGTYNSRD ESTDSGLSKS SYSPRTPDD FLUSVDHDT GOTTSQSTLP SQQSRFPDVL EALPCTINVL GTLEGDAMI
1:461 to 488	EGEELPSPQL DALSSLELQV ESNLAATKLD KESFLTW

**Figure 4. Detection and identification of alternative splicing forms of YAP1**

(A) Western blotting analysis of pregnant embryo for YAP1. (B) Antibody epitope site in mouse YAP1 protein. (C-F) Western blot analysis revealed bands at 70 kDa, 60 kDa, 52 kDa, and 28 kDa, which were further analyzed and compared with the YAP1 sequence using LC-MS/MS.

### **Protein expression profiles of YAP1 during early pregnancy**

Uterine proteins from early pregnant mice were analyzed by western blotting using YAP1 antibody, and the intensity of the bands observed in Figure 2 was quantified for profiling. The band detected around 70 kDa showed a significant increase on day 7 of pregnancy compared to days 1, 2, 4, and 5 (Fig. 5A). The band around 60 kDa showed a significant increase on days 6 and 7 compared to day 1, and also showed a significant increase compared to all subsequent days starting from day 2 (Fig. 5B). The band around 52 kDa showed a significant increase on days 4 and 7 compared to day 1, and day 7 exhibited a significantly higher intensity compared to all earlier days (Fig. 5C). The band around 28 kDa showed a significant increase on days 3, 4, and 7 compared to day 1, with day 7 showing a significantly higher intensity compared to all other time points (Fig. 5D). The integrated intensity of all four bands showed a sharp increase on day 7, which was significantly higher than all previous time points (Fig. 5E).

The wet weight of half of the uterus extracted for protein analysis was measured, showing a significant increase starting on day 5 of pregnancy, with a sharp increase on day 7 (Fig. 5F).

These results indicate that there is a positive correlation between the expression level of YAP1 and the increase in uterine size and weight during pregnancy in mice. This suggests that YAP1 may play a role in processes such as cell proliferation in the pregnant uterus.

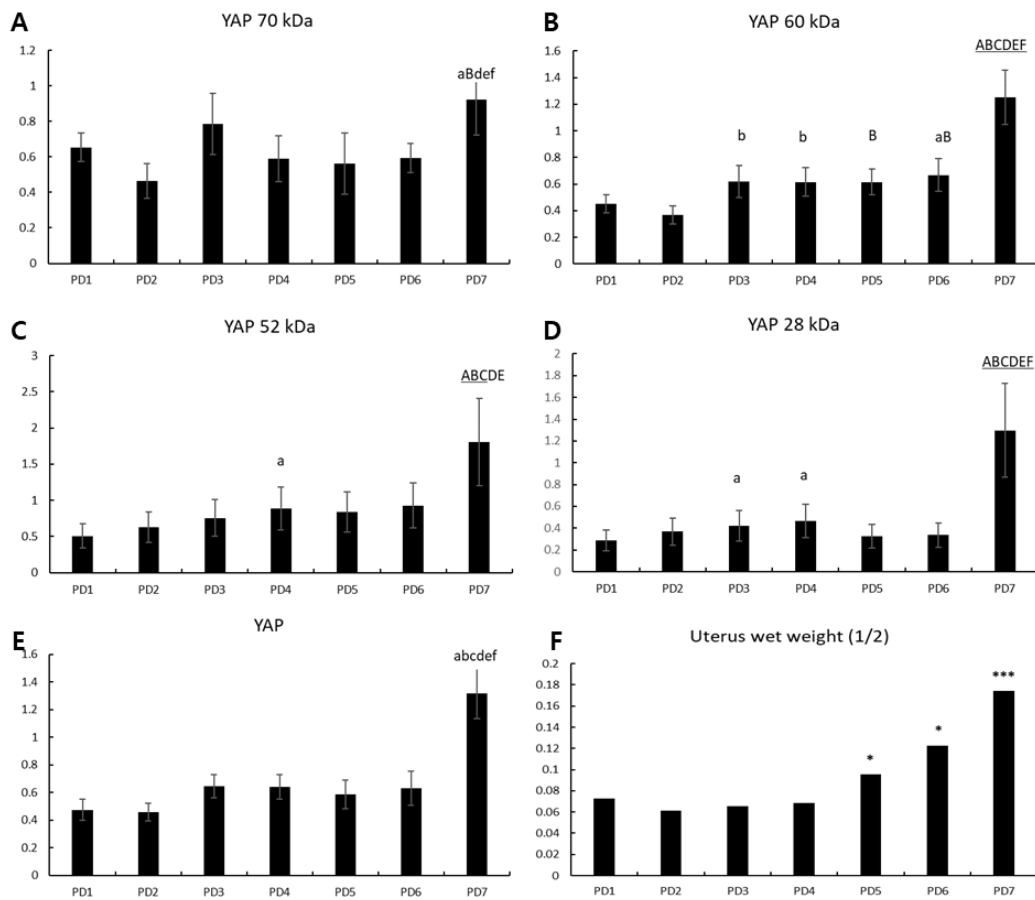


**Figure 5. Protein expression profiles of YAP1 during early pregnancy.**

Western blot analysis of mouse uterus in pregnant day 1 to 7. The target protein levels were normalized to GAPDH. Intensity is measured using the ImageJ system. a:  $p < 0.05$  (a significant difference vs PD1). b:  $p < 0.05$  (a significant difference vs PD2). c:  $p < 0.05$  (a significant difference vs PD3). d:  $p < 0.05$  (a significant difference vs PD4). e:  $p < 0.05$  (a significant difference vs PD5). f:  $p < 0.05$  (a significant difference vs PD6). In the notation of statistical significance, uppercase letters represent  $p < 0.01$ , and underlining denotes  $p < 0.001$ . \*:  $p < 0.05$  (a significant difference vs PD1). \*\*\*:  $p < 0.001$  (a significant difference vs PD1). Data are represented as the mean  $\pm$  SEM.

### **Increase of the levels of YAP1 protein by implantation**

Uterine tissue from pregnant mice on day 7, after the removal of the myometrium, was collected and divided into implantation and inter-implantation sites for protein extraction (Fig. 6A). Western blotting was performed on the extracted proteins using YAP1 antibody. Analysis of the band intensities for the 70 kDa, 60 kDa, 52 kDa, and 28 kDa bands showed that all bands had significantly higher expression in the implantation site compared to the inter-implantation site (Fig. 6B).

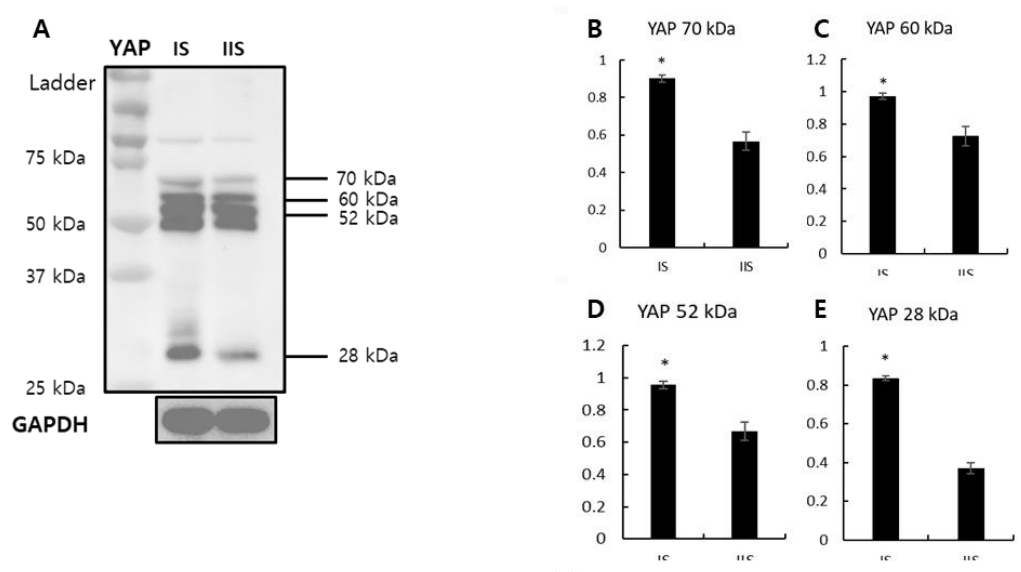


**Figure 6. Increase of the levels of YAP1 protein by implantation.**

Western blot analysis of implantation site and inter-implantation site of mouse uterus removed myometrium in pregnant day 7. The target protein levels were normalized to GAPDH. Intensity is measured using the ImageJ system. \*:  $p < 0.05$  (implantation site vs inter-implantation site). IS: implantation site. IIS: inter-implantation site.

### **Glycosylated YAP1 during pregnancy**

To confirm whether the size discrepancy of the four detected bands was due to size missing from PTM, we performed deglycosylation on proteins extracted from the uterus of pregnant mice. The enzymes used for this process were PNGase F, which specifically cleaves N-glycans, and a deglycosylating enzyme mix, which cleaves both N-glycans and O-GlcNAc (Fig. 7A). Fetuin, a control protein that undergoes both N-glycosylation and O-glycosylation, was subjected to deglycosylation with each enzyme. After SDS-PAGE, PNGase F-treated Fetuin showed a reduced size of approximately 15 kDa, and Fetuin treated with the deglycosylating enzyme mix showed a reduction to approximately 18 kDa, confirming effective deglycosylation (Fig. 7B). After performing deglycosylation on proteins extracted from the uterus of day 7 pregnant mice, western blot analysis with a YAP1 antibody revealed the disappearance of a band around 60 kDa (Fig. 7C), suggesting that the 60 kDa band represents glycosylated YAP1.

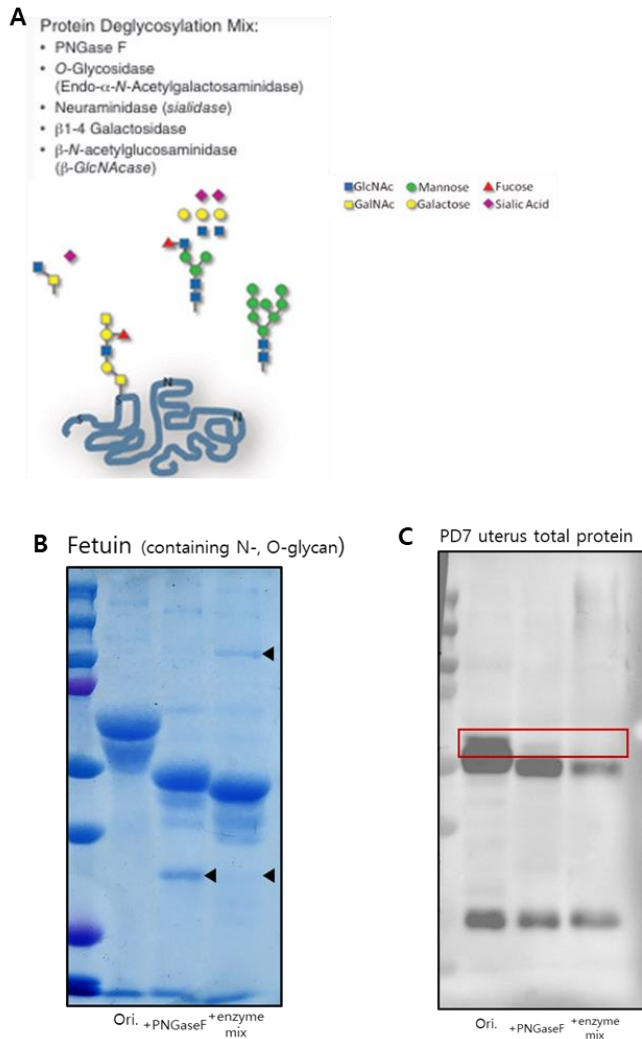


**Figure 7. Glycosylated YAP1 during pregnancy.**

(A) The enzymes included in the deglycosylation enzyme mix and their mechanisms. (B) After deglycosylating fetuin and total protein from the uterus of pregnant mice on pregnant day 7, SDS-PAGE was performed, and the gel was stained with Coomassie Blue. The arrow heads indicate the bands corresponding to the deglycosylating enzymes. (C) After deglycosylating total protein from the uterus of pregnant mice on day 7, Western blotting was performed to detect YAP1.

## **O-GlcNAcylation in mouse YAP1**

O-GlcNAcylation, a form of O-glycosylation, is a post-translational modification (PTM) in which O-GlcNAc is attached to the serine or threonine residues of proteins, and it dynamically changes depending on the cellular energy state. Recent studies have shown that human YAP1 undergoes O-GlcNAcylation, which competitively inhibits its phosphorylation, promotes YAP1's translocation into the nucleus, and consequently enhances its transcriptional coactivator activity. The site of phosphorylation in human YAP1 and the site where O-GlcNAc competes for binding is serine 109, which corresponds to serine 94 in mouse YAP1, based on a conserved sequence. Using the O-GlcNAcAtlas 3.0 program, the O-GlcNAcylation site in mouse YAP1 was identified at serine 94 (Table 5). This suggests that, similar to humans, O-GlcNAcylation at serine 94 may promote YAP1's transcriptional coactivator function in mice, prompting further investigation into YAP1 O-GlcNAcylation in the uterus of pregnant mice.

Western blot analysis using an O-GlcNAc antibody on proteins extracted from the uterus of mice from day 1 to day 7 of pregnancy revealed a tendency for increased O-GlcNAcylated protein levels as pregnancy progressed (Fig. 8A, 8B).

Additionally, immunoprecipitation of YAP1 using a YAP1 antibody followed by western blotting with an O-GlcNAc antibody on proteins extracted from the uterus of pregnant mice on days 3 and 7 showed that the 52 kDa and 28 kDa bands of YAP1 were found to interact with O-GlcNAc, as confirmed by co-immunoprecipitation (co-IP) analysis (Fig. 8C).

**Table 5. O-GlcNAcylation sites in mouse YAP1.**

Using the O-GlcNAcAtlas 3.0 program, the O-GlcNAcylation sites of mouse YAP1 were identified (Ma et al., 2021).

ID	Peptide Seq	Site Residue	Position in Peptide	Position in Protein	Method	Species	Sample Type	Data Source PMID
6433	QASTDAGTAGALTPQHVR	S	3	94	MS	mouse	embryonic fibroblasts	32782141
6438	QASTDAGTAGALTPQHVR	T	8	99	MS	mouse	embryonic fibroblasts	32782141
6647	TMTTNSDPFLNSGTYHSR	T	1	361	MS	mouse	embryonic fibroblasts	32782141
6649	TMTTNSDPFLNSGTYHSR	T	3	363	MS	mouse	embryonic fibroblasts	32782141
1E+07	TMTTNSDPFLNSGTYHSR	T	4	364	MS	mouse	embryonic fibroblasts	32782141

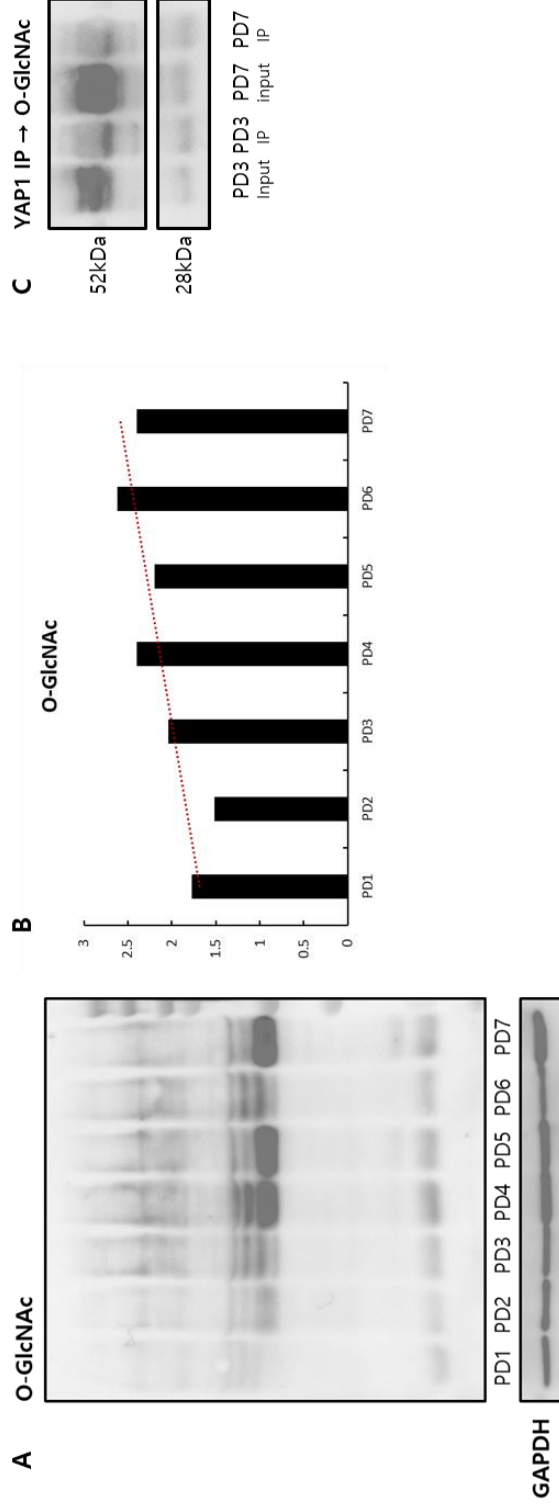


**Figure 8. O-GlcNAcylation in mouse YAP1**

(A, B) Western blot analysis of mouse uterus in pregnant day 1 to 7. The target protein levels were normalized to GAPDH. Intensity is measured using the ImageJ system. (C) Co-immunoprecipitation experiments in mice uterus at pregnant day 3 and 7. Western blot analysis was performed on both the input and immunoprecipitated (IP) proteins using antibodies specific to the indicated proteins. The input sample included 7% of the total amount of recombinant proteins used for co-immunoprecipitation.

## DISCUSSION

In this study, the role of YAP1 was investigated in the uterus during early pregnancy and how its alternative splicing forms and O-GlcNAcylation impact uterine decidualization. The results suggest that YAP1 plays a crucial role in the uterus during early pregnancy. Notably, the expression of YAP1 undergoes significant changes during the decidualization process, and it was confirmed that alternative splicing and O-GlcNAcylation can influence this process.

First, YAP1 expression exhibited dramatic fluctuations at key points during early pregnancy, coinciding with periods of active decidualization on days 5 and 7. This suggests that YAP1 plays a significant role during decidualization. Additionally, the level of YAP1 expression correlated with the increase in uterine size and weight, which implies that YAP1 is involved in important processes such as uterine cell proliferation. This finding contrasts with a previous study where no significant difference in decidual response was observed between normal mice and AMHR-based conditional YAP1 null mice following artificial decidual induction. However, the conditional YAP1 null mouse model used in that study (Amhr2-IRES-Cre(Bhr)/+ mouse model) has a mosaic nature that leads to widespread gene recombination or Cre activity leakage (Dickson et al., 2023) suggesting that the observed normal decidualization in this model was erroneous.

Second, several alternative splicing forms of YAP1 identified. These alternative splicing forms of YAP1 could generate proteins of various sizes and functions, offering the possibility that YAP1 is regulated diversely within the uterus during both decidualization and pregnancy. In particular, the splicing of YAP1 may vary depending on the characteristics of uterine cells, highlighting the need for

further studies to understand how different YAP 1 isoforms contribute to the decidualization process.

Third, it was observed that O-GlcNAcylation of YAP1 plays an important role in the activation of YAP1 during early pregnancy. To determine if YAP1 is regulated by post-translational modifications (PTMs), we tracked changes in YAP1 through glycosylation and examined YAP1's interaction with O-GlcNAc using co-immunoprecipitation (co-IP). Our findings confirmed that O-GlcNAcylation significantly affects YAP1 modification and activation. Specifically, our results align with previous studies showing that O-GlcNAcylation promotes YAP1 nuclear activation by competing with LATS1/2-mediated phosphorylation.

Finally, it is intriguing that the expression of YAP1 and the levels of O-GlcNAcylation are closely linked with various physiological changes during early pregnancy. This suggests that YAP1 plays an essential role in transcriptional activation during decidualization, with regulation related to the cell's energy state fine-tuning YAP1's function. YAP1 appears to be a critical protein not only for decidualization but also for proper uterine response during early pregnancy. However, this finding contrasts with a previous study in which O-GlcNAcylated protein levels were found to decrease over time in cultured mouse endometrial stromal cells undergoing decidualization induction (Muter et al., 2018). Therefore, it is necessary to experimentally verify this discrepancy through in vitro culture experiments to determine whether the conflicting results arise due to differences between in vitro and in vivo conditions.

Additionally, based on the results, it can propose conducting in vitro culture experiments where YAP1 agonists and antagonists are separately applied during the decidualization process, along with treatment of OGT (which induces O-GlcNAcylation) and OGA (which removes O-GlcNAcylation). This will allow us to

accurately determine the roles of YAP1 and O-GlcNAcylated YAP1 during the decidualization process.

In summary, our findings confirm that the alternative splicing forms and O-GlcNAcylation of YAP1 play significant roles in YAP1 activation and decidualization in the uterus during early pregnancy. This study provides valuable information that can deepen our understanding of YAP1's role and potentially lead to new therapeutic approaches for ensuring the successful progression of pregnancy.

## REFERENCES

- Chen, H., Song, Y., Yang, S., Fu, J., Feng, X., & Huang, W. (2017). YAP mediates human decidualization of the uterine endometrial stromal cells. *Placenta*, *53*, 30-35. <https://doi.org/10.1016/j.placenta.2017.03.013>
- Chen, Y.-A., Lu, C.-Y., Cheng, T.-Y., Pan, S.-H., Chen, H.-F., & Chang, N.-S. (2019). WW Domain-Containing Proteins YAP and TAZ in the Hippo Pathway as Key Regulators in Stemness Maintenance, Tissue Homeostasis, and Tumorigenesis [Review]. *Frontiers in Oncology*, *9*. <https://doi.org/10.3389/fonc.2019.00060>
- Dickson, M. J., Gruzdev, A., & DeMayo, F. J. (2023). iCre recombinase expressed in the anti-Müllerian hormone receptor 2 gene causes global genetic modification in the mouse. *Biology of Reproduction*, *108*(4), 575-583. <https://doi.org/10.1093/biolre/ioad012>
- Godin, P., Tsoi, M., Paquet, M., & Boerboom, D. (2020). YAP and TAZ are required for the postnatal development and the maintenance of the structural integrity of the oviduct. *Reproduction*, *160*(2), 307-318. <https://doi.org/10.1530/rep-20-0202>
- Han, X., Li, X., Liu, H., Zhang, H., Li, A., Dong, M., Xu, Y., Yan, B., Sui, L., & Kong, Y. (2019). O-GlcNAc modification influences endometrial receptivity by promoting endometrial cell proliferation, migration and invasion. *Oncol Rep*, *42*(5), 2065-2074. <https://doi.org/10.3892/or.2019.7317>
- He, J. P., Tian, Q., Zhu, Q. Y., & Liu, J. L. (2021). Identification of Intercellular Crosstalk between Decidual Cells and Niche Cells in Mice. *Int J Mol Sci*, *22*(14). <https://doi.org/10.3390/ijms22147696>
- Kim, M. K., Jang, J. W., & Bae, S. C. (2018). DNA binding partners of YAP/TAZ. *BMB Rep*, *51*(3), 126-133. <https://doi.org/10.5483/bmbrep.2018.51.3.015>
- Ma, J., Li, Y., Hou, C., & Wu, C. (2021). O-GlcNAcAtlas: A database of experimentally identified O-GlcNAc sites and proteins. *Glycobiology*, *31*(7), 719-723. <https://doi.org/10.1093/glycob/cwab003>

- Mannino, M. P., & Hart, G. W. (2022). The Beginner's Guide to O-GlcNAc: From Nutrient Sensitive Pathway Regulation to Its Impact on the Immune System. *Front Immunol*, *13*, 828648. <https://doi.org/10.3389/fimmu.2022.828648>
- Meng, Z., Moroishi, T., & Guan, K. L. (2016). Mechanisms of Hippo pathway regulation. *Genes Dev*, *30*(1), 1-17. <https://doi.org/10.1101/gad.274027.115>
- Moon, S., Lee, O. H., Kim, B., Park, J., Hwang, S., Lee, S., Lee, G., Kim, H., Song, H., Hong, K., Cho, J., & Choi, Y. (2022). Estrogen Regulates the Expression and Localization of YAP in the Uterus of Mice. *Int J Mol Sci*, *23*(17). <https://doi.org/10.3390/ijms23179772>
- Muter, J., Alam, M. T., Vrljicak, P., Barros, F. S. V., Ruane, P. T., Ewington, L. J., Aplin, J. D., Westwood, M., & Brosens, J. J. (2018). The Glycosyltransferase EOGT Regulates Adropin Expression in Decidualizing Human Endometrium. *Endocrinology*, *159*(2), 994-1004. <https://doi.org/10.1210/en.2017-03064>
- Paria, B. C., Huet-Hudson, Y. M., & Dey, S. K. (1993). Blastocyst's state of activity determines the "window" of implantation in the receptive mouse uterus. *Proc Natl Acad Sci U S A*, *90*(21), 10159-10162. <https://doi.org/10.1073/pnas.90.21.10159>
- Peng, C., Zhu, Y., Zhang, W., Liao, Q., Chen, Y., Zhao, X., Guo, Q., Shen, P., Zhen, B., Qian, X., Yang, D., Zhang, J. S., Xiao, D., Qin, W., & Pei, H. (2017). Regulation of the Hippo-YAP Pathway by Glucose Sensor O-GlcNAcylation. *Mol Cell*, *68*(3), 591-604.e595. <https://doi.org/10.1016/j.molcel.2017.10.010>
- Sudol, M. (2013). YAP1 oncogene and its eight isoforms. *Oncogene*, *32*(33), 3922-3922. <https://doi.org/10.1038/onc.2012.520>
- Vassilev, A., Kaneko, K. J., Shu, H., Zhao, Y., & DePamphilis, M. L. (2001). TEAD/TEF transcription factors utilize the activation domain of YAP65, a Src/Yes-associated protein localized in the cytoplasm. *Genes Dev*, *15*(10), 1229-1241. <https://doi.org/10.1101/gad.888601>

- Wang, H., & Dey, S. K. (2006). Roadmap to embryo implantation: clues from mouse models. *Nature Reviews Genetics*, 7(3), 185-199. <https://doi.org/10.1038/nrg1808>
- Xu, Y., Wang, X., Yu, M., Ruan, Y., Zhang, J., Tian, Y., Xiong, J., Liu, L., Cheng, Y., Yang, Y., Ren, B., Chen, G., Zhang, Y., Zhao, B., Wang, J., Wang, J., Jian, R., Liu, Y., & Wang, J. (2021). Identification, subcellular localization, and functional comparison of novel Yap splicing isoforms in mouse embryonic stem cells. *IUBMB Life*, 73(12), 1432-1445. <https://doi.org/10.1002/iub.2571>
- Yu, H. F., Yang, Z. Q., Xu, M. Y., Huang, J. C., Yue, Z. P., & Guo, B. (2022). Yap is essential for uterine decidualization through Rrm2/GSH/ROS pathway in response to Bmp2. *Int J Biol Sci*, 18(6), 2261-2276. <https://doi.org/10.7150/ijbs.67756>
- Zhao, B., Kim, J., Ye, X., Lai, Z. C., & Guan, K. L. (2009). Both TEAD-binding and WW domains are required for the growth stimulation and oncogenic transformation activity of yes-associated protein. *Cancer Res*, 69(3), 1089-1098. <https://doi.org/10.1158/0008-5472.Can-08-2997>

## 논문개요

Decidualization은 초기 임신 과정에서 배아 착상과 발달을 지원하기 위해 자궁 내막 기질 세포가 분화하는 중요한 과정입니다. Hippo signaling pathway는 세포 증식, 생존 및 세포 자살에 관여하는 serine/threonine kinase 신호 전달 경로로, 발생 과정과 암 진행에서 중요한 역할을 하는 인자로 인식되고 있습니다. 본 연구에서는 Hippo signaling pathway의 주요 효과자인 YAP1이 초기 임신 중 decidualization에서 어떤 역할을 하는지 조사하였습니다. YAP1, 그 타겟 유전자 CTGF, 그리고 YAP1과 상호작용하는 TEAD 전사인자들에 대한 웨스턴 블롯 분석을 통해 YAP1, CTGF, TEAD1의 발현이 decidualization이 진행됨에 따라 증가하는 것을 확인했습니다. 면역조직화학적 분석에서는 임신 1일차부터 7일차까지 decidualization 진행에 따라 YAP1의 국소화가 동적으로 변화하는 것을 확인할 수 있었습니다. 또한, 웨스턴 블롯 분석에서 YAP1의 alternative splicing form에 해당하는 네 개의 뚜렷한 밴드를 확인하였고, 임신 7일차에서 발현이 유의미하게 증가했으며, 이는 자궁 크기와 무게의 증가와 상관관계를 보였습니다. 또한, 착상 부위에서 비착상 부위보다 YAP1의 발현이 더 높게 나타나 YAP1이 착상에 중요한 역할을 한다는 것을 확인할 수 있었습니다. 후속 실험을 통해 YAP1의 post-translational modifications(PTMs)에 미치는 영향을 조사한 결과, 60 kDa 밴드가 당화된 YAP1에 해당하는 것으로 나타났습니다. 추가적으로, O-GlcNAcAtlas 3.0 프로그램을 사용하여 마우스 YAP1의 O-GlcNAcylation이 94번 세린에서 일어난다는 사실을 확인했으며, 이는 인간 YAP1과 유사한 양상으로 YAP1의 전사 공동활성화 기능을 조절할 수 있음을 시사합니다. 또한 임신 초기 마우스의 자궁에서 O-GlcNAcylation 된 단백질의 수준을 western blot을 통해 확인하였을 때 임신 1일차에서 7일차까지 점진적으로 증가하는 경향을 보였고, co-IP 분석 결과를 통해 52kDa과 28kDa의

YAP1에 O-GlcNAc에 결합함을 확인하였습니다. 본 연구는 YAP1이 초기 임신 자궁에서 세포 증식과 분화에 중요한 역할을 하며, O-GlcNAcylation과 같은 PTM이 YAP1의 기능을 조절할 수 있음을 제시합니다.

## 감사의 글

학부연구생 시기부터 석사 학위 과정을 마무리하기까지, 짧지 않은 4 년의 시간 동안 많은 분들의 가르침과 격려가 있었습니다. 이 자리를 빌어 감사의 마음을 전하고자 합니다.

먼저 석사과정을 잘 마무리할 수 있도록 지도와 격려, 칭찬을 아끼지 않으신 전용필 교수님께 감사드립니다. 실험적으로 어려움을 겪고 있을 때면 바쁘실텐데도 바로 장갑 끼고 찾아와주시고, 스스로에 대한 확신을 가지지 못하고 있을 때면 조목조목 근거를 들어 저를 믿어주셨던 교수님 덕분에 많은 성장을 이룰 수 있었습니다.

또한 논문을 완성하는 데에 있어 많은 도움과 아이디어 주신 이성호 교수님, 질량분석 실험을 진행하면서 실험적으로 많은 도움과 조언 주신 고병준 교수님과 윤서 쌤, 학부시절 생물학에 발을 디는 데에 많은 가르침을 주셨던 성신여자대학교 바이오생명공학과 교수님들과, 석사과정 동안 학문의 깊이를 키우는 데에 큰 가르침을 주신 금동호 교수님, 김정훈 교수님, 김수아 박사님께도 감사드립니다.

먼저 석사과정을 경험하신 선배님으로서 많은 공감과 조언, 응원해주신 오화순 박사님과 황희경 박사님! 석사 생활뿐 아닌 이후 취업 관련해서도 많은 정보와 도움 주셔서 감사드립니다. 강의를 함께 수강할 수 있어 너무 감사했고, 함께했던 식사자리들이 모두 너무 맛있고 따뜻했어요!

항상 유쾌하고 화끈했던 JS 메이트 지선언니와, 첫 후배라면서 맨날 끼고 다니며 꼬박꼬박 밥 사 먹여 키워준 내 귀인 보영언니랑 내 이상형 정빈언니!! 실험에 있어서도 정말 많이 배웠고, 랩실 생활하는 동안 너무 많은 추억 쌓게 해준 장본인들이십니다. 언니들 후배라서 너무너무 즐거웠으니 앞으로도 책임지고 자주 놀아주길..♡

학부연구생 시절 동안 모든 실험과 고민을 함께 해준 수호림 멤버 유림&지호, 든든한 대학원 동기이자 유쾌하고 따뜻한 왕언니인 인하언니, 내 처음이자 마지막 대학원 후배 주희지야! 랩실 생활을 함께하는 동지들이 있어서 의지가 많이 됐다! 언젠가 제가 도움될 수 있는 일이 있다면 연락주세요!

내가 랩실 결정하는 데에 결정적인 역할을 해주고 매일매일 하루종일을 함께 랩실 생활했던 예림아, 매일 볼 수는 없었지만 같이 석사 생활하면서 주기적으로 만나 근황 나눠준 은우야! 대학입학부터 대학원 졸업까지 너희랑 함께 할 수 있어서 너무

감사하구 다행이야. 방학마다 만나서 근황 나누고 여행 다닌 게 큰 힘이 되더라. 앞으로도 셋이 자주 만나 놀러다니면서 서로 리프레쉬 시켜주자!

여전하게 연락하고 종종 만나 고등학생때와 다름없이 먹고 놀아주는 다은이 환이 현진이 예진이 은숨이 보은이도 너무 고마워. 앞으로도 알지?

항상 끝없는 응원과 지지와 기도로 힘이 되어 준 예인교회 청대에도 감사드립니다.

마지막으로 본가도 잘 안 오고 연락도 먼저 잘 안 하는 딸이라 항상 먼저 전화해주고 찾아와주는 엄마아빠! 언제나 믿어주고 지지해주고 기도해주셔서 감사하고 사랑해요. 종종 깜짝용돈 쥐어주는 지후니도 땡큐. 언제나 귀여워주는 초코&치즈도 덕분에 힐링 많이 했다! 이제 자주 놀러갈 테니 더 자주 오래 보자!

감사의 말을 전하지 못한 모든 분들께도 진심으로 감사의 마음을 전합니다.

작년까지만해도 논문이란 걸 써낼 수 있을까 걱정만 가득했는데, 많은 분들의 도움을 받아 어느덧 학위논문을 완성하여 학위를 받을 수 있었습니다. 앞으로도 이 배움과 경험을 바탕으로 성장하는 사람이 되겠습니다.